Combining Multibody Dynamics, Finite Elements Method and Fluid Film Lubrication to Describe Hermetic Compressor Dynamics

ILMAR SANTOS[1] and EDGAR ESTUPINAN[2]
Technical University of Denmark
Department of Mechanical Engineering
Nils Koppels Allé 404, 2800 Kgs. Lyngby
DENMARK

Abstract: This work describes in details the steps involved within the mathematical modelling of reciprocating linear compressors. The dynamics of the mechanical components are described with help of Dynamics of Multibody Systems (rigid components) and Finite Element Method (flexible components). Some of the mechanical elements are supported by fluid film bearings where the hydrodynamics interaction forces are described by Reynolds equation. Two approaches are investigated, i.e. short and infinite long bearings. The system of nonlinear equations are numerically solved, taking into account the lateral and tilting vibration of the centre of the crank. The behaviour of the orbits in the journal bearings is presented giving some insights into design parameters, as maximal oil film pressure, minimum oil film thickness and maximum vibration levels.

Key–Words: Hermetic compressor, multibody dynamics, journal bearings, Reynolds equation, finite elements.

1 Introduction

Small-scale hermetic reciprocating compressors are widely used to compress coolant gas in household refrigerators and air-conditioners. Almost since the 60's these small machines became a necessary appliance in every household in the industrialized countries. Since then, a lot of research has been done to optimize the design and to improve the thermal and mechanical efficiency. Reciprocating compressors use pistons that are driven directly through a slider-crank mechanism, converting the rotating movement of the rotor to an oscillating motion. In this type of compressors, motor and compressor are directly coupled on the same shaft and the assembly is installed inside a welded steel shell. Figure 1, shows a schematic view of an hermetic reciprocating compressor used in household refrigerators.

The study and optimization of the dynamic behaviour of reciprocating compressors, taking in account the hydrodynamics of bearings is of significant importance for the development of new prototypes. The performance of the bearings affects key functions such as durability, noise and vibration of the compressor. Optimization of the behaviour of journal bearings by means of numerical simulation may reduce development costs for prototype testing work significantly.

Several computational models for the analysis of small reciprocating compressors can be found in the literature. They range from simple simulations including steady-state energy balance until more complex models of unsteady analysis of the heat and work transfer and thermal and fluid dynamic analysis. A complete literature review of previous studies with focus on compressor simulation models is included in [9]. Some of these studies require numerical simulations of the refrigerant flow through the valves and inside the cylinder during the compression cycle [7], whereas other studies focus mainly on the dynamics of motion in steady and transient conditions [2]. For instance, a study that included the coupling of fluid-structure dynamics to analyse the dynamics of piston is presented in [1]. In a study carried out by Kim and

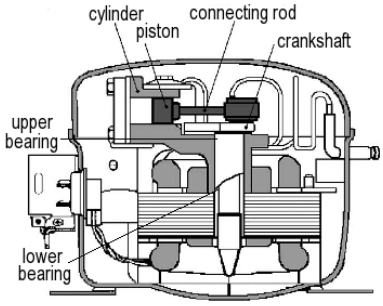

Figure 1: Hermetic reciprocating compressor

Han [3], an analytical model of the coupled dynamic behaviour of the piston and crankshaft was developed and comparisons between a finite bearing model and a short bearing approach were included. Additionally, a numerical procedure combining Newton-Raphson method and the Successive Over Relaxation scheme was also presented. In the study carried out by Cho and Moon [1], a time-incremental numerical algorithm to solve a finite differences model for the estimation of the oil film pressure is coupled with a finite element model for the computation of the structural deformation of the piston. Although most of the work done related to modelling of compressors is related to the thermal and fluid dynamic behaviour, in this work the main focus and contribution are on the developing of a multibody dynamic model that represents the dynamics of the main mechanical components of hermetic compressors. This model is coupled with a finite element model of the rotor, where the hydrodynamic interaction forces are computed using analytical solutions of Reynolds equation. The elastohydrodynamic theory, which takes in account the bearing and housing flexibility is not considered in this paper, since it is presented only in very special cases.

2 Mathematical modelling

In this section the formulation of representative equations describing the mathematical simulation model for a hermetic compressor is developed. The motion of the piston has been modelled as particle, the motion of the connecting rod and crank as rigid bodies and the shaft is modelled as a flexible body via finite elements.

Nomenclature

A_p	:	transversal area of the piston
c_b	:	clearance of bearing
h_b	:	oil film thickness
h_p	:	length of pin connection crank-connecting rod
l	:	length of the connecting rod
l_b	:	width of bearing
m_c	:	mass of the crank
m_{cr}	:	mass of the connecting rod
m_p	:	mass of the piston
P_g	:	pressure inside the cylinder
r_b	:	radio of bearing
r_c	:	Radius crank-pin center
T_z	:	motor shaft torque
Ω	:	rotational speed of the rotor $[rpm]$
θ	:	rotation angle of the crank
α	:	rotation angle of the connecting rod
μ	:	viscosity oil film
ϕ	:	attitude angle
x_C,y_C	:	displacements in *X*, *Y* directions of crank center
x_B	:	displacement of the piston in *X*-direction
$\bar{\mathbf{r}}_{\mathbf{cr}}$	:	vector of position, center of mass connecting rod
$\mathbf{F_A}$	:	vector of reaction forces in pin crank-connecting rod
$\mathbf{F_B}$	:	vector of reaction forces in pin piston-connecting rod

2.1 Developing of the multibody dynamics model

The motion equations for the piston-connecting rod-crank system are formulated using the Newton-Euler's method. Figure 2a shows a sketch indicating the inertial referential frame system XYZ and the main angles of rotation for the moving reference systems.

(a) Definition of the inertial and moving reference systems. One inertial reference system $I(XYZ)$ and four moving reference systems have been defined. The moving references systems B_1, B_2 and B_3 are attached to the crank to describe the tilting and rotational movement of the crank and the moving reference system B_4 is attached to the connecting rod.

B_1 $(X_1Y_1Z_1)$, is obtained by rotating I the angle β around X axis.
B_2 $(X_2Y_2Z_2)$, is obtained by rotating B_1 the angle Γ around Y_1 axis.
B_3 $(X_3Y_3Z_3)$, is obtained by rotating B_2 the angle θ around Z_2 axis.
B_4 $(X_4Y_4Z_4)$, is obtained by rotating I the angle α around Z axis.

The transformation matrices are given by:

$\mathbf{T}_\beta$: transformation from the inertial frame I to the moving frame B_1.
$\mathbf{T}_\Gamma$: transformation from the inertial frame B_1 to the moving frame B_2.
$\mathbf{T}_\theta$: transformation from the inertial frame B_2 to the moving frame B_3.
$\mathbf{T}_\alpha$: transformation from the inertial frame I to the moving frame B_4.

(b) Position vectors and constraint equations. This model takes into account lateral displacements and tilting oscillations of the centre of the crank. Figure 2b shows a simplified sketch illustrating how the basic elements of the system are connected. The constraint equation is given by:

$$ {}_I\mathbf{X_p} + {}_I\mathbf{L} = {}_I\mathbf{R} + {}_I\mathbf{C} \tag{1}$$

$$ {}_\mathbf{I}\mathbf{X_p} = \begin{Bmatrix} \mathbf{x_B} \\ 0 \\ -h_p \end{Bmatrix} \; ; \; {}_\mathbf{I}\mathbf{L} = \begin{Bmatrix} -l\cos\alpha \\ l\sin\alpha \\ 0 \end{Bmatrix} \; ; \; {}_\mathbf{I}\mathbf{C} = \begin{Bmatrix} x_C \\ y_C \\ 0 \end{Bmatrix} \; ; $$

$$ {}_I\mathbf{R} = \mathbf{T}_\beta^\mathbf{T}\mathbf{T}_\Gamma^\mathbf{T}\mathbf{T}_\theta^\mathbf{T}{}_{\mathbf{B_3}}\mathbf{R} \quad ; \quad {}_{\mathbf{B_3}}\mathbf{R} = \begin{Bmatrix} r_c & 0 & -h_p \end{Bmatrix}^\mathbf{T} $$

(c) Kinematic relations.The absolute angular velocity (ω) written with help of the moving reference frame B_3, is given by:

$$ {}_{B_3}\boldsymbol{\omega} = {}_{B_3}\dot{\boldsymbol{\beta}} + {}_{B_3}\dot{\Gamma} + {}_{B_3}\dot{\boldsymbol{\theta}} \tag{2}$$

where:

$ {}_{B_3}\dot{\boldsymbol{\beta}} = \mathbf{T}_\theta\mathbf{T}_\Gamma\mathbf{T}_{\beta\,I}\dot{\boldsymbol{\beta}}$; ${}_{B_3}\dot{\Gamma} = \mathbf{T}_\theta\mathbf{T}_{\Gamma\,B_1}\dot{\Gamma}$ and ${}_{B_3}\dot{\boldsymbol{\theta}} = \mathbf{T}_{\theta\,B_2}\dot{\boldsymbol{\theta}}$

The expressions to calculate the velocity and acceleration of the piston ($\dot{x}_B$ and $\ddot{x}_B$) as well as the angular velocity and acceleration of the connecting rod ($\dot{\alpha}$ and $\ddot{\alpha}$), are obtained differentiating once and twice the constraint equation (1), obtaining:

- Velocities:

$$ \begin{bmatrix} 1 & l\sin\alpha \\ 0 & l\cos\alpha \end{bmatrix} \begin{Bmatrix} \dot{x}_B \\ \dot{\alpha} \end{Bmatrix} = \begin{Bmatrix} v_1 \\ v_2 \end{Bmatrix} \tag{3}$$

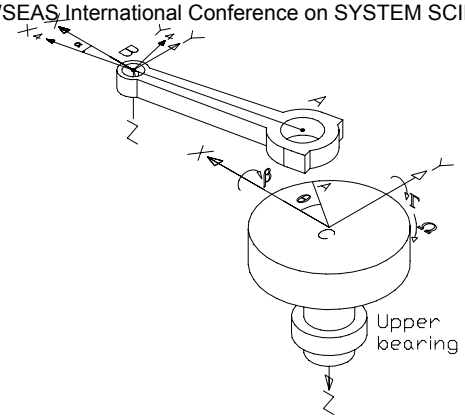

(a) Inertial and moving reference systems

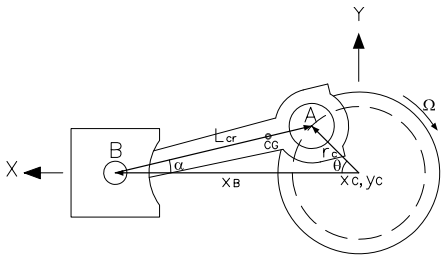

(b) Piston - connecting rod - crank system

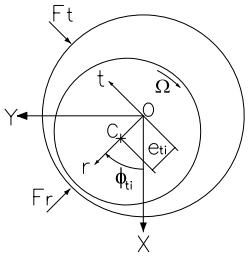

(c) Journal bearing geometry

Figure 2: Geometry and reference systems

- Accelerations:

$$\begin{bmatrix} 1 & l\sin\alpha \\ 0 & l\cos\alpha \end{bmatrix} \begin{Bmatrix} \ddot{x}_B \\ \ddot{\alpha} \end{Bmatrix} = \begin{Bmatrix} a_1 \\ a_2 \end{Bmatrix} \tag{4}$$

where:

$$\begin{aligned}
v_1 &= -r_c(\dot{\Gamma}s\Gamma c\theta + \dot{\theta}c\Gamma s\theta) - h_p\dot{\Gamma}c\Gamma + \dot{x}_C \\
v_2 &= r_c\dot{\beta}(c\beta s\Gamma c\theta - s\beta s\theta) + r_c\dot{\theta}(c\beta c\theta - s\beta s\Gamma s\theta) \\
&\quad +\dot{\Gamma}(r_c s\beta c\Gamma c\theta - h_p s\beta s\Gamma) + \dot{\beta}h_p c\beta c\Gamma + \dot{y}_C \\
a_1 &= -r_c\ddot{\Gamma}s\Gamma c\theta + \dot{\Gamma}^2(h_p s\Gamma - r_c c\Gamma c\theta) + 2r_c\dot{\theta}\dot{\Gamma}s\Gamma s\theta \\
&\quad -r_c\dot{\theta}^2 c\Gamma c\theta - h_p\ddot{\Gamma}c\Gamma - r_c\ddot{\theta}c\Gamma s\theta - l\dot{\alpha}^2 c\alpha + \ddot{x}_C \\
a_2 &= -r_c\dot{\theta}^2(c\beta s\theta + s\beta s\Gamma c\theta) - \dot{\beta}^2(r_c c\beta s\theta + r_c s\beta s\Gamma c\theta + h_p s\beta c\Gamma) \\
&\quad -\dot{\Gamma}^2(r_c s\beta s\Gamma c\theta + h_p s\beta c\Gamma) + \ddot{\beta}(h_p c\beta c\Gamma - r_c s\beta s\theta + r_c c\beta s\Gamma c\theta) \\
&\quad +\ddot{\Gamma}(r_c s\beta c\Gamma c\theta - h_p s\beta s\Gamma) - 2r_c\dot{\theta}\dot{\beta}(s\beta c\theta + c\beta s\Gamma s\theta) \\
&\quad +2\dot{\beta}\dot{\Gamma}(r_c c\beta c\Gamma c\theta - h_p c\beta s\Gamma) - 2r_c\dot{\theta}\dot{\Gamma}s\beta c\Gamma s\theta \\
&\quad +r_c\ddot{\theta}(c\beta c\theta - s\beta s\Gamma s\theta) + l\dot{\alpha}^2 s\alpha + \ddot{y}_C
\end{aligned}$$

In these equations: $s\theta = \sin\theta;\ c\theta = \cos\theta;\ s\alpha = \sin\alpha;$ $c\alpha = \cos\alpha;\ s\beta = \sin\beta;\ c\beta = \cos\beta;\ s\Gamma = \sin\Gamma;\ c\Gamma = \cos\Gamma.$

(d) Equations of motion. Using Newton-Euler's method, the equations of motion for each body are:

Force Equation - Crank

$$\sum {}_I\mathbf{F} = m_c \cdot_I \bar{\mathbf{a}}_c = {}_I\mathbf{F_A} = m_c \left\{ \begin{array}{ccc} \ddot{x}_C & \ddot{y}_C \end{array} \right\}^T \tag{5}$$

Moment Equation - Crank

$$\begin{aligned}
&\sum {}_{B_3}\mathbf{M_O} = {}_{\mathbf{B3}}\,\mathbf{r} \times_{\mathbf{B3}} \mathbf{F_A} + {}_{\mathbf{B3}}\,\mathbf{T_m} = {}_{\mathbf{B_3}}\,\mathbf{I_O}\frac{\mathbf{d}}{\mathbf{dt}}\left({}_{\mathbf{B_3}}\boldsymbol{\omega}\right) \\
&+ {}_{B_3}\,\boldsymbol{\omega} \times \left({}_{B_3}\mathbf{I}_O \cdot_{B_3} \boldsymbol{\omega}\right) + m_c \cdot_{B_3} \bar{\mathbf{r}}_{C-cm} \times_{B_3} \mathbf{a}_O \\
&{}_{B3}\mathbf{F_A} = \mathbf{T}_\theta \cdot \mathbf{T}_\Gamma \cdot \mathbf{T}_\beta \cdot_{\mathbf{I}} \mathbf{F_A} \qquad (6) \\
&{}_{B3}\mathbf{T_m} = \left\{ \begin{array}{ccc} 0 & 0 & T_z \end{array} \right\}^T \quad {}_{B_3}\bar{\mathbf{r}}_{C-cm} = \left\{ \begin{array}{ccc} e_c & 0 & 0 \end{array} \right\}^T
\end{aligned}$$

Force Equation - Connecting rod

$$\sum {}_I\mathbf{F} = m_{cr} \cdot_I \bar{\mathbf{a}}_{cr} = {}_I\mathbf{F_A} + {}_I\mathbf{F_B} \tag{7}$$

Moment Equation - Connecting rod

$$\begin{aligned}
&\sum {}_{B_4}\mathbf{M_B} = {}_{\mathbf{B4}}\,\mathbf{l} \times_{\mathbf{B4}} \mathbf{F_A} = {}_{\mathbf{B_4}}\,\mathbf{I_{cr}} \cdot \frac{\mathbf{d}}{\mathbf{dt}}\left({}_{\mathbf{B_4}}\dot{\boldsymbol{\alpha}}\right) + \\
&{}_{B_4}\dot{\boldsymbol{\alpha}} \times \left({}_{B_4}\mathbf{I}_{cr} \cdot_{B_4} \dot{\boldsymbol{\alpha}}\right) + m_{cr} \cdot_{B_4} \bar{\mathbf{r}}_{\mathbf{cr}} \times_{B_4} \mathbf{a}_B \qquad (8) \\
&{}_{B4}\mathbf{F_A} = \mathbf{T}_\alpha \cdot_{\mathbf{I}} \mathbf{F_A};\ \ {}_{\mathbf{B4}}\mathbf{a_B} = \mathbf{T}_\alpha \cdot_{\mathbf{I}} \mathbf{a_B}
\end{aligned}$$

Force Equation - Piston

$$\begin{aligned}
&\sum {}_I\mathbf{F_B} = m_p \cdot_I \mathbf{a}_B = {}_I\mathbf{F_B} + {}_I\mathbf{N} + {}_I\mathbf{F_p} \qquad (9) \\
&{}_I\mathbf{F_p} = \left\{ \begin{array}{ccc} P_g \cdot A_p, & 0 & 0 \end{array} \right\}^T
\end{aligned}$$

The equations of motion for the multibody dynamic model in a matrix form may be written as in (10). In order to solve this matrix system, taking into account the lateral and tilting vibration of the crank, this matrix system has to be coupled with the equations of the finite element model of the rotor, which will be explained in detail in section 3.

$$\begin{aligned}
&\bar{\mathbf{A}} \times \bar{\mathbf{f}} = \bar{\mathbf{C}} \qquad (10) \\
&\bar{\mathbf{f}} = \{f_{B_x}, f_{B_y}, f_{B_z}, N_y, N_z, f_{A_x}, f_{A_y}, f_{A_z}, \\
&\quad f_{c_z}, \ddot{\theta}, \ddot{x}_B, \ddot{\alpha}, \ddot{x}_C, \ddot{y}_C, \ddot{\beta}, \ddot{\Gamma}\}^T
\end{aligned}$$

2.2 Modelling of the rotor

The main rotor-shaft of the compressor, which drives the crank-connecting rod-piston system is modelled as a flexible body via finite elements method [8]. The global equation of motion can be written as:

$$\bar{\bar{\mathbf{M}}} \cdot \ddot{\mathbf{q}} = \bar{\bar{\mathbf{Q}}} - \bar{\bar{\mathbf{D}}} \cdot \dot{\mathbf{q}} - \bar{\bar{\mathbf{K}}} \cdot \mathbf{q} \tag{11}$$

where, $\bar{\bar{\mathbf{Q}}} = {}_{\mathbf{pl}}\mathbf{Q} + {}_{\mathbf{ub}}\mathbf{Q} + {}_{\mathbf{b}}\mathbf{Q}$. In this vector, ${}_{\mathbf{pl}}\mathbf{Q}$ is the vector of static preload forces, ${}_{\mathbf{ub}}\mathbf{Q}$ is the vector of rotor unbalance forces and ${}_{\mathbf{b}}\mathbf{Q}$ is the vector of dynamic journal bearing forces.

2.3 Fluid film forces

The governing equation (12) for the pressure distribution of the oil film in dynamically loaded journal bearings may be obtained from the general formulation of Reynolds equation [4]. In this equation, $\dot{\phi}$ is the rotational speed of the journal centre about the bearing centre and ϵ is the relative eccentricity. The fluid film thickness is calculated using: $h_b = c_b(1 + \epsilon \cos\varphi)$, where φ is the angle measured from the location of the maximum film thickness. Figure 2c, illustrates the main geometrical relations of a journal bearing.

$$\frac{\partial}{\partial\varphi}\left(\frac{{h_b}^3}{\mu}\frac{\partial p}{\partial\varphi}\right) + {r_b}^2\frac{\partial}{\partial z}\left(\frac{{h_b}^3}{\mu}\frac{\partial p}{\partial z}\right) = 12{c_b}{r_b}^2\left[\frac{\partial\epsilon}{\partial t}\cos\varphi + \epsilon\sin\varphi(\dot{\phi} - \frac{\Omega}{2})\right] \tag{12}$$

With dynamically loaded bearings the eccentricity and attitude angle will vary through the loading cycle. The pressure generated when a journal bearing is dynamically loaded can be determined if the normal squeeze velocity ($\frac{\partial\epsilon}{\partial t}$) and the rotational velocities $\dot{\phi}$ and Ω are known at any eccentricity ratio [4]. Complete solutions of equation (12) may be obtained numerically, and solutions for limited cases may be also obtained analytically. In this paper analytical solutions for the short-bearing and infinity long-bearing theories have been used. The short-journal-bearing theory assumes that the variation of pressure is more significant in the axial direction than in the circumferential direction and therefore the first term in equation (12) is neglected. In contrast, for an infinitely long-journal-bearing solution the pressure in the axial direction is assumed to be constant, therefore, the side-leakage term, i.e. the second term in (12), is neglected. For each one of these two particular cases, the reduced Reynolds equation can be integrated analytically and the pressure can be computed [5]. The journal bearing forces in r, t coordinates can be calculated integrating the pressure distribution. If the analysis is limited to the convergent film ($0 \leq \varphi \leq \pi$), this solution is known as a half Sommerfeld solution. In real bearings lower pressures than the ambient pressure are rarely found, therefore, using this approach more realistic predictions may be obtained [4]. The analytical expressions used in this paper to calculate the radial and transversal forces using the half Sommerfeld conditions are given in [5].

3 Numerical implementation

The equation of motions for each connected body of the multibody system together with the FEM model of the shaft and the analytical expressions for the fluid film forces yield to a system of high complexity and non-linearity. The numerical algorithm developed to solve this system is shown in figure 3. Considering that the system has a "stiff" behaviour because of the combination of a rigid body model with a finite element model, a Newmark implicit method combined with a predictor-corrector approach is used [6]. The simulation procedure is summarized in the following four main steps:

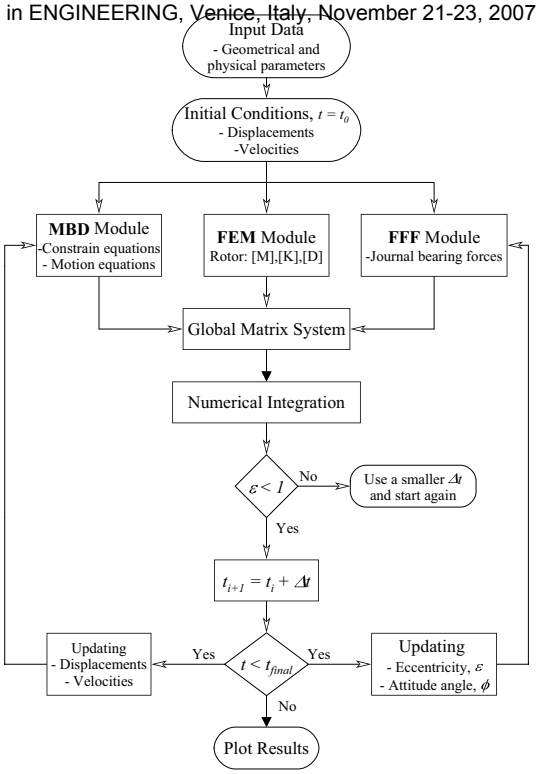

Figure 3: Flowchart for the numerical computer code

- a) Input data and starting values. In this part all of the geometrical and physical parameters are given, i.e. dimensions, rotational speed, mass, inertia, preloads, etc. Initial displacements and initial velocities should be also given here.
- b) Pre-processing. This step includes the generation of structural matrices for the MBD system (MBD module) and the matrices of the flexible rotor (FEM module). In this part initial fluid film forces may be computed with the FFF module, based on the initial conditions.
- c) Numerical computation. This part includes the coupling of matrices, the computation of the journal bearing forces at each time step and the numerical solution of the global system. At each time step, new fluid film forces are computed, using the analytical solutions of Reynolds equation and they are included in the global matrix system (13) where the equilibrium has to be achieved. To couple the MBD matrix system (10) to the matrices of the flexible rotor (11),

the matrix $\bar{\mathbf{M}}$ of size $ndof \times ndof$ is coupled to the matrix $\bar{\mathbf{A}}$ of size 16×16 in the degrees of freedom related to the linear and angular accelerations of the crank center node ($\ddot{q}_1, \ddot{q}_2, \ddot{q}_3, \ddot{q}_4$), obtaining the global mass matrix $\hat{\mathbf{M}}$ of dimension $ndof + 12$. Similarly, the resultant right hand side vector of equation (11) is coupled to the vector $\bar{\mathbf{C}}$ of equation (10). The global matrix system may be expressed as in (13). The initial forces and accelerations ($\hat{\mathbf{f}}_\mathbf{0}, \ddot{\mathbf{q}}_\mathbf{0}$) are calculated from $\hat{\mathbf{M}}^{-1}_{\mathbf{t_0}} \times \hat{\mathbf{Q}}_{\mathbf{t_0}}$. The iterative equations are given by (14), (15) and (16).

$$\hat{\mathbf{M}} \cdot \{\hat{\mathbf{f}}, \ddot{\mathbf{q}}\}^{\mathbf{T}} = \hat{\mathbf{Q}} \tag{13}$$

$$\hat{\mathbf{f}} = \{f_{B_x}, f_{B_y}, f_{B_z}, N_y, N_z, f_{A_x}, f_{A_y}, f_{A_z}, f_{c_z}, \ddot{\theta}, \ddot{x}_B, \ddot{\alpha}\}^T$$
$$\ddot{\mathbf{q}} = \{\ddot{q}_1, \ddot{q}_2, ..., \ddot{q}_{ndof}\}^T$$

$$\{\hat{\mathbf{f}}_{\mathbf{t_{i+1}}}, \ddot{\mathbf{q}}_{\mathbf{t_{i+1}}}\}^{\mathbf{T}} = \hat{\mathbf{M}}^{-1}_{\mathbf{t_{i+1}}} \times \hat{\mathbf{Q}}_{\mathbf{t_{i+1}}} \tag{14}$$

$$\dot{q}_{t_{i+1}} = \dot{q}_{t_i} + h\left[(1-\hat{\gamma})\ddot{q}_{t_i} + \hat{\gamma}\ddot{q}_{t_{i+1}}\right] \tag{15}$$

$$q_{t_{i+1}} = q_{t_i} + h\dot{q}_{t_i} + \frac{h^2}{2}\left[(1-2\hat{\beta})\ddot{q}_{t_i} + 2\hat{\beta}\ddot{q}_{t_{i+1}}\right] \tag{16}$$

To compute $\ddot{q}_{t_{i+1}}$, the load vector $\hat{\mathbf{Q}}_{\mathbf{t_{i+1}}}$ must be estimated previously, which implies to calculate the vector of journal bearing forces ${}_\mathbf{b}\mathbf{Q}_{\mathbf{t_{i+1}}}$ that depends on the positions and velocities at the time t_{i+1}. Therefore, initial values for $\ddot{q}^0_{t_{i+1}}$ and $q^0_{t_{i+1}}$ are predicted with the Heun's explicit method. Then, using (14) $\ddot{q}^1_{t_{i+1}}$ can be initially estimated and $\dot{q}^1_{t_{i+1}}$ and $q^1_{t_{i+1}}$ using (15) and (16) can be respectively calculated. These new estimated values can be used to update the journal bearing forces and using again (14) a new estimation of $\ddot{q}^2_{t_{i+1}}$ can be obtained, and so on until the difference of two consecutive values is smaller than a prescribed tolerance. The explicit Euler method of first order is used at each iteration to estimate the crank angle θ_{t_i} and the instantaneous angular velocity $\dot{\theta}_{t_i}$ from $\ddot{\theta}_{t_i}$, which is contained in vector $\hat{\mathbf{f}}$ in (14).

• d) The last step is post-processing, which includes the generation of plots of journal bearing orbits, journal bearing forces, maximal oil film pressure and minimum fluid film thickness.

4 Analysis of the Results

The main geometrical dimensions and physical properties of the reciprocating compressor used for the numerical simulations are given in table 1. The curve of gas pressure (P_g) as function of the crank angle, which is used for the simulations, is presented in [1]. The data of torque variation as function of the angular velocity, is taken from an experimental curve for a typical motor of an hermetic compressor, obtained in [9]. An initial rotational speed of $2990rpm$ and a preload on the bearings in X-direction of $85N$, were given.

Table 1: Geometrical and physical parameters

Radius crank-pin centre	$r_c = 7.5mm$
Radius and width of bearings	$r_b = 8mm$; $l_b = 8mm$
Journal clearance	$c_b = 15\mu m$
Distance between bearings	$L = 80mm$
Mass moment of inertia	$I_x = I_y = 0.4 \times 10^{-3} kg.m^2$
of motor rotor	$I_z = 0.1 \times 10^{-2} kg.m^2$
Diameter of piston	$D_p = 23mm$ ($A_p = 415.5mm^2$)
Mass of the piston	$m_p = 0.043kg$
Lubricant viscosity	$\mu = 0.005Pa.s$

Figure 4 shows the orbits obtained for the upper bearing and lower bearing considering different bearing clearances and using the short bearing approach. It can be seen that the damping effect of the oil film decreases as the clearance of the journal increases. Figure 5 shows the dynamic journal bearing forces and the fluid film thickness for the upper bearing as function of the crankshaft angle. It can be seen that the force in X-direction follows a similar pattern to the profile of the pressure inside the cylinder. The minimum film thickness is obtained at each revolution, when the piston is close to the top dead centre. Figure 6 is a plot of the maximum pressures in the oil film. From the results it is possible to conclude that the value of the maximum journal pressure is more than six times bigger than the pressure inside the cylinder. The maximum pressure and minimum oil film thickness are found during the compression cycle when the piston starts to move back to the bottom dead centre, i.e. after the beginning of the expansion cycle. In figure 7a, a comparison between the journal forces for a short and long journal bearing approach is carried out, showing only small differences between the two

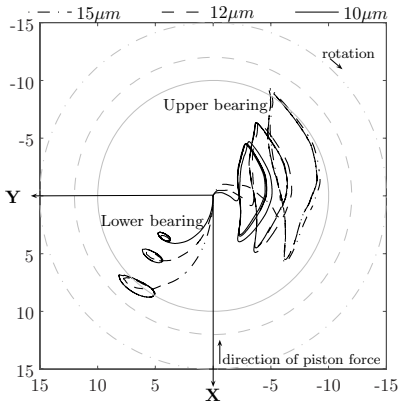

Figure 4: Orbits using different journal bearing clearances, c_b. (a) $-\cdot-$ 15μm, (b)$--$ 12μm, (c) — 10μm

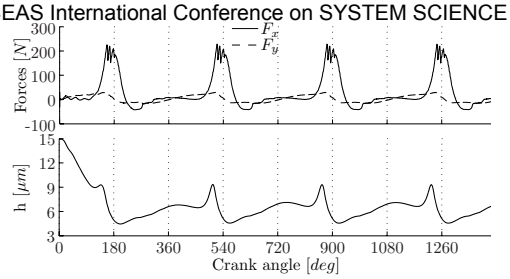

Figure 5: Upper journal bearing forces and minimum film thickness as a function of the crank angle.

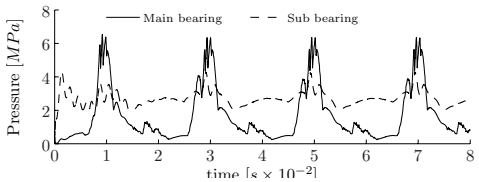

Figure 6: Maximum pressure in the journal bearings

approaches. Figure 7b show the minimum film thickness obtained for both cases, and it can be seen that there is only a small difference in the minimum value found during each revolution. However, when the piston is not close to the point of maximum pressure, the long bearing approach predicts thicker oil films.

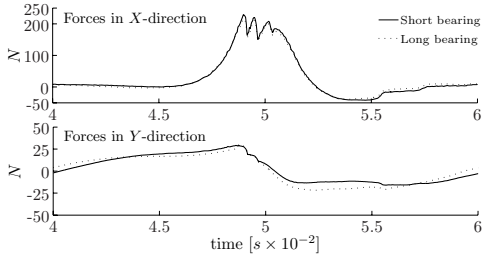

(a) Journal bearing forces

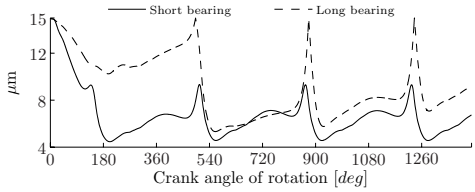

(b) Minimum film thickness

Figure 7: Comparison between the short-bearing and long-bearing approach for the upper journal bearing

5 Conclusion

In the model analyzed of a hermetic compressor, the lateral and tilting vibrations of the crank have been included. Therefore and considering that the oil film thickness is only a few micrometers thick, more precise estimations of the journal bearing forces and minimum film thickness are obtained. Good agreement for the calculation of forces and minimum film thickness have been found for both cases, i.e. short and long bearing approaches. The simulations were carried out for bearings with a width to radius ratio equal to 1. In such a case, the discrepancies between the two approaches are of the order of 20% for the minimum film thickness. The maximum forces and the minimum film thickness are obtained when the piston is close to the top dead center. It is important to point out that there is a delay between the maximum journal pressure and the minimum oil film thickness.

Acknowledgements: Supported by the Programme Alβan of the EU, scholarship No. E06D101992CO.

References:

[1] J.R. Cho and S.J. Moon, A numerical analysis of the interaction between the piston oil film and the component deformation in a reciprocating compressor, *Tribology International*, 38, 2005, pp. 459-468.

[2] R. Dufour, J. Der Hagopian and M. Lalanne, Transient and steady state dynamic behaviour of single cylinder compressors: prediction and experiments, *Journal of Sound and Vibration*, 181, 1995, pp. 23-41.

[3] T.J. Kim and J.S. Han, Comparison of the dynamic behavior and lubrication characteristics of a reciprocating compressor crankshaft in both finite and short bearing models, *Tribology Transactions*, 47-1, 2004, pp. 61-69.

[4] B. J. Hamrock, *Fundamental of Fluid Film Lubrication*, NASA Reference Publication, USA, 1991.

[5] J. Frêne, D. Nicolas and others, *Lubrification Hydrodynamique* Editions Eyrolles, Paris, 1990.

[6] J.Garcia de Jalon and E. Bayo. *Kinematic and Dynamic Simulation of Multibody Systems.*. Springer-Verlag, New-York, 1994.

[7] G. Longo and A. Gasparella, Unsteady state analysis of the compression cycle of a hermetic reciprocating compressor, *International Journal of Refrigeration*, 26, 2003, pp. 681-689.

[8] H. D. Nelson, A finite rotating shaft element using Timoshenko beam theory, *Journal of Mechanical Design*, 102, 1980, pp. 793-803.

[9] J. Rigola, *Numerical simulation and experimental validation of hermetic reciprocating compressors*, Doctoral Thesis. Universidad Politécnica de Cataluña. Spain, 2002.